Showcasing research from Professor Sotiris K. Hadjikakou's laboratory of Biological Inorganic Chemistry, Department of Chemistry, University of Ioannina, Greece.

Tetracycline: structural characterization and antimicrobial properties of its water-soluble di-anionic bi-sodium salt

One of the most pressing contemporary issues faced by any healthcare system is the emergence of microbial resistance to modern antibiotics. Despite being an older, well-established antibiotic, tetracycline continues to be widely utilized across many healthcare systems. Recently, in our laboratory, we have enhanced the efficacy of tetracycline by modifying its structure, thereby increasing its potency against both gram-positive and gram-negative microbes.

This paper was supported by the Special Account for Research Funds (Research Committee) of the University of Ioannina

As featured in:

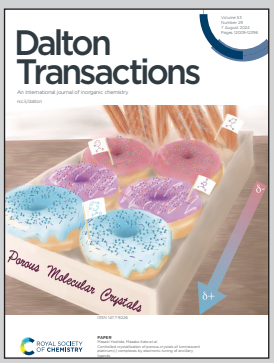

See Christina N. Banti, Sotiris K. Hadjikakou *et al.*, *Dalton Trans.*, 2024, **53**, 12080.

ROYAL SOCIETY OF CHEMISTRY

rsc.li/dalton

Registered charity number: 207890

Dalton Transactions

ROYAL SOCIETY OF CHEMISTRY

PAPER

View Article Online
View Journal | View Issue

Cite this: *Dalton Trans.*, 2024, **53**, 12080

Tetracycline: structural characterization and antimicrobial properties of its water-soluble di-anionic bi-sodium salt†

Afroditi S. Tsigara,[a] Christina N. Banti, *[a] Antonios Hatzidimitriou[b] and Sotiris K. Hadjikakou *[a]

Received 10th May 2024,
Accepted 23rd May 2024

DOI: 10.1039/d4dt01384k

rsc.li/dalton

The new water-soluble di-anionic bi-sodium salt of tetracycline (TC), an antibiotic in clinical use, with the formula $\{[TC]^{2-}[Na^{+}(MeOH)(H_2O)]\ [Na^{+}]\cdot(H_2O)\}_n$ (**TCNa**) was synthesized. The compound was characterized by m.p., attenuated total reflectance-Fourier transform infra-red (ATR-FTIR) spectroscopy, and ultraviolet (UV) and proton nuclear magnetic resonance (^{1}H NMR) spectroscopy in the solid state and in solution. The molecular weight (MW) was determined by cryoscopy. The crystal structure of **TCNa** was also determined by X-ray crystallography. The antibacterial activity of **TCNa** was evaluated against the bacterial species *Pseudomonas aeruginosa* (*P. aeruginosa*), *Escherichia coli* (*E. coli*), *Staphylococcus epidermidis* (*S. epidermidis*) and *Staphylococcus aureus* (*S. aureus*) by means of minimum inhibitory concentration (MIC), minimum bactericidal concentration (MBC) and inhibition zones (IZs). Moreover, the ability of the compound to eradicate biofilm formation was also evaluated. The results are compared with those obtained for the commercially available drug **TCH$_2$**. The *in vitro* and *in vivo* toxicities of **TCNa** were tested against human corneal epithelial cells (HCECs) and *Artemia salina*.

Introduction

Tetracycline is a widely used antibiotic with a broad spectrum of bactericidal properties against both Gram-positive and Gram-negative bacteria.[1,2] Tetracyclines, initially employed as topical drops and ointments, represent a group of antibiotics utilized in the treatment of blepharitis.[3] In particular, tetracycline ointment continues to be utilized as a treatment for trachoma (chlamydial infections) due to its status as the sole topical treatment available for numerous years.[4] The current applications of tetracycline include both therapy and prophylaxis against human infections such as ocular diseases.[5] In particular, tetracycline is used in the treatment or inhibition of corneal ulceration.[6] Recently, an ophthalmic solution containing tetracycline was patented against eye surface inflammation.[7] Although tetracycline is usually available as a peroral drug only, it is characterized by low hydrophilicity and poor absorption after administration.[8] One of the methods used to overcome its low solubility in water is its hydrochlorination.[9] As has already been highlighted, bacteria have acquired resistance to tetracyclines.[10] Consequently, it is imperative to advance the development of novel tetracycline-based antibiotics capable of addressing the challenge posed by bacterial resistance. Tetracycline derivatives exhibit multiple functional groups (Scheme 1, labeled A–D) that can serve as potential ligand sites for complex formation leading to novel antibiotics.

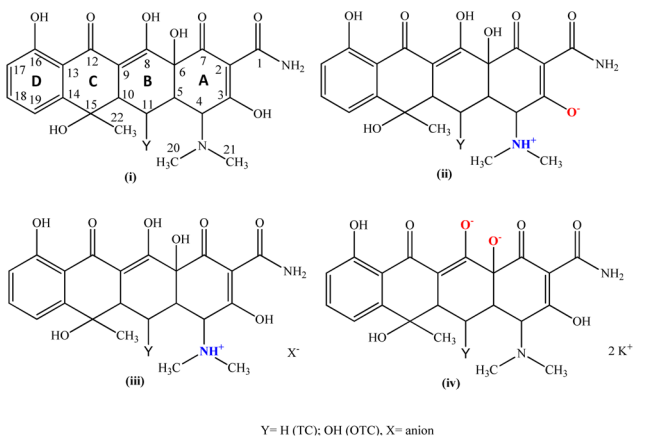

Scheme 1 The structural motifs of oxy-tetracyclines, OTCs, (Y = OH) (neutral (i), zwitterionic (ii), cationic (iii) and dianionic (iv)) and the corresponding ones of tetracycline (TC) Y = H (zwitterionic (ii) and cationic (iii)).

[a]*Biological Inorganic Chemistry Laboratory, Department of Chemistry, University of Ioannina, 45110 Ioannina, Greece. E-mail: cbanti@uoi.gr, shadjika@uoi.gr; Tel: +xx30-26510-08374*

[b]*Laboratory of Inorganic Chemistry, Department of Chemistry, Aristotle University of Thessaloniki, Greece*

†Electronic supplementary information (ESI) available. CCDC 2330616. For ESI and crystallographic data in CIF or other electronic format see DOI: https://doi.org/10.1039/d4dt01384k

Four main types of oxy-tetracycline (OTC) moieties have been found and characterized by X-ray analysis to date. These include the (i) neutral tetracyclines (Scheme 1),[11,12] (ii) zwitterionic tetracyclines (Scheme 1),[11,13–16] (iii) cationic tetracyclines (Scheme 1)[17–20] and (iv) di-anionic tetracyclines (Scheme 1).[13]

However, only zwitterionic and cationic structures of tetracyclines have been reported to date: (ii) zwitterionic tetracyclines (Scheme 1)[11,14–16] and (iii) cationic tetracyclines (Scheme 1).[17,18,21]

During our investigations into the design and creation of innovative formulations aimed at overcoming bacterial resistance experienced by existing antibiotics,[22–30] we have successfully synthesized and characterized a modified version of the commercially available drug tetracycline (TCH_2 = tetracycline) (Scheme 1). The crystal structure of {$[TC]^{2-}[Na^+(MeOH)(H_2O)][Na^+]\cdot(H_2O)$} (**TCNa**) was refined from an X-ray diffraction data set. **TCNa** was characterized by melting point (m.p.) and ATR-FTIR, ^{1}H-NMR and UV–vis spectroscopic techniques. The molecular weight of the compound was determined by cryoscopy in solution. The Gram-negative strains *Pseudomonas aeruginosa* (*P. aeruginosa*) and *Escherichia coli* (*E. coli*), as well as the Gram-positive bacteria, including *Staphylococcus epidermidis* (*S. epidermidis*) and *Staphylococcus aureus* (*S. aureus*), prevalent in microbial keratitis, were subjected to an assessment of the antibacterial activity of **TCNa**. In order to accomplish this, we assessed the minimum inhibitory concentration (MIC), minimum bactericidal concentration (MBC), and inhibition zone (IZ). Additionally, we evaluated the impact of **TCNa** on the formation of biofilm by both *Staphylococcus aureus* (*S. aureus*) and *Pseudomonas aeruginosa* (*P. aeruginosa*). The *in vitro* toxicity of **TCNa** was estimated using normal human corneal epithelial cells (HCECs). Additionally, the *Artemia salina* model was employed to evaluate the *in vivo* toxicity of **TCNa**.

Results and discussion

General aspects

Tetracycline reacts with sodium hydroxide (NaOH) in the presence of carbon disulfide (CS_2) in methanol (MeOH) in a 1 : 3 : 3 molar ratio (Scheme 2). The yellow precipitate was crystallized by slow evaporation of MeOH solution. **TCNa** is stable when it is stored under ambient conditions in the dark and it is soluble in H_2O, MeOH, MeCN, DMSO and acetone. The water solubility of **TCNa** was verified using UV–vis spectroscopy. Fig. S1† illustrates the UV–vis spectra of **TCNa** in water.

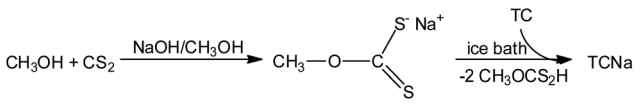

Scheme 2 Synthetic route of **TCNa**.

Solid state studies

Crystal and molecular structure of TCNa. A molecular diagram of **TCNa** along with selected bond lengths and angles are shown in Fig. 1.

Thus far, only the zwitterionic form of tetracycline (TC) has been documented. In contrast, oxytetracycline (OTC) has exhibited a broader range of crystallized forms, including neutral, zwitterionic, cationic, and di-anionic, all characterized by X-ray crystallography.[11–16,19] While the dianionic oxytetracycline (OTC) in the potassium salt form has been previously

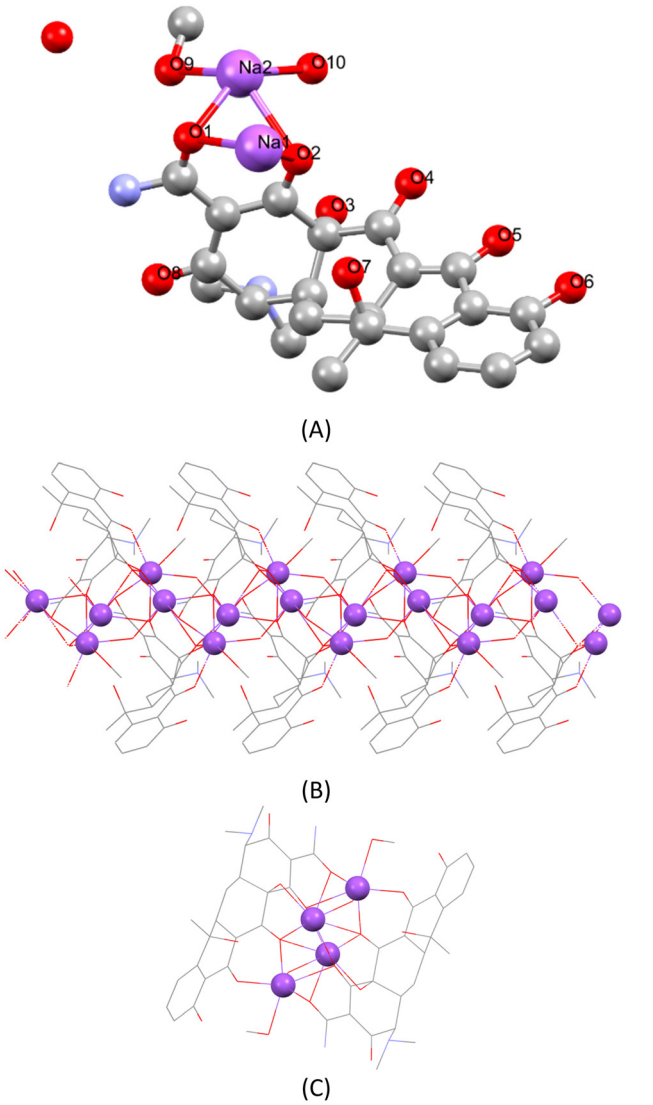

Fig. 1 (A) Molecular diagram of **TCNa**. Selected bond lengths (Å) and angles [°]: Na1–O1: 2.444(3), Na1–O2: 2.462(3), Na2–O1: 2.256(2), Na2–O2: 2.530(3), Na2–O9: 2.464(3), Na2–O10: 2.306(3), O9–C23: 1.428(4), O1–C1: 1.236(3), O2–C7: 1.235(3), O3–C6: 1.401(3), O4–C8: 1.285(3), O5–C12: 1.259(3), O6–C16: 1.340(3), O7–C15: 1.449(3), O1–Na1–O2: 65.03(7), O1–Na2–O2: 66.58(7), Na2–O9: 93.29(8), O1–Na2–O10: 140.71(8), O2–Na2–O9: 125.98(8), O2–Na2–O10: 80.33(7), O9–Na2–O10: 89.35(8); 1D-ribbon supramolecular assembly along the *a*-axis (B) and the *b*-axis (C).

reported by Jogun *et al.*,[13] with the formula $\{(OTC)^{2-}2(K^{1+})2(H_2O)2(CH_3OH)\}$, the **TCNa** $\{[TC]^{2-}[Na^{+}(MeOH)(H_2O)][Na^{+}]\cdot(H_2O)\}_n$ represents the first reported example of a di-anionic and non-zwitterionic form for tetracycline itself. Table 1 provides a summary of the reported C–O bond lengths for both tetracycline (TC) and oxytetracycline (OTC) across various forms documented thus far. Table 2 presents a compilation of the average bond lengths of C1–O, C3–O, C4–O, and C13–O measured so far for both tetracycline (TC) and oxy-tetracycline (OTC) in their reported forms (neutral, zwitterionic, cationic, and dianionic).

The asymmetric unit of **TCNa** includes one TC^{2-} ion, which interacts with two Na^{+} ions through the oxygen atom of the amide bond and the corresponding one of the A-ring (Scheme 1 and Fig. 1A). Two consequent $\{[TC]^{2-}[Na^{+}(MeOH)(H_2O)][Na^{+}]\cdot(H_2O)\}$ units form a dimer, which are linked to each other *via* ten Na–O contacts, involving four sodium cations and two TC molecules. Finally, a 1D ribbon supramolecular assembly of the covalent polymer $\{[TC]^{2-}[Na^{+}(MeOH)(H_2O)][Na^{+}]\cdot(H_2O)\}_n$ is established although an extended network is formed, held together by Na–O contacts ranging from 2.256 to 2.767 Å, ensuring that all Na atoms are 6-coordinated (Fig. 1B and C). This extended network of Na–O contacts, however, affects the C–O bond lengths, rendering their comparison (in Tables 1 and 2) pointless.

Vibrational spectroscopy. The $\nu(H–C_{aromatic})$ and $\nu(H–C_{aliphatic})$ band vibrations in the FTIR spectrum of TCH_2 and **TCNa** are observed at 3063–3048, 2955, and 2925 cm^{-1} and at 3070, 2936, and 2920 cm^{-1}, respectively[29,31,32] (Fig. S2†). The vibrational bands at 1639 and 1599 cm^{-1} in the FTIR spectrum of TCH_2 are assigned to the amide $\nu(O{=}C(1))$ and $\nu(O{=}C(7))$ bond vibrations, respectively (Scheme 1).[29,31,32] These bands are shifted at 1674 and 1609 cm^{-1}, respectively, in the spectrum of **TCNa**. The pronounced change is a result of tetracycline coordinating with Na^{+} *via* the O(C1) and O(C7) atoms. The vibration band at 1397 cm^{-1} is attributed to $\nu(O–C(8))$, which is shifted at 1419 cm^{-1} in the spectrum of **TCNa**. This is a consequence of the deprotonation of the hydroxyl group at the C(8) position, leading to an increase in the bond order of the C(8)–O bond. The vibrational band observed at 1302 cm^{-1} in the IR spectrum of TCH_2 is assigned to the $\nu(O–C(3))$ bond, while in the case of **TCNa**, a slight shift is observed at 1297 cm^{-1}.

Table 2 C1–O, C3–O, C4–O and C13–O average bond lengths (Å) found in TCs and OTCs, respectively

Type	C1–O (Å)	C3–O (Å)	C4–O (Å)	C13–O (Å)
Neutral	1.272 ± 0.004	1.231 ± 0.004	1.339 ± 0.003	1.305 ± 0.002
Zwitterionic	1.255 ± 0.009	1.238 ± 0.005	1.334 ± 0.007	1.245 ± 0.011
Cationic	1.333	1.235	1.356	1.264
Di-anionic	1.236 ± 0.000	1.248 ± 0.025	1.272 ± 0.026	1.261 ± 0.020

Solution studies

Molecular weight (MW) measurement. The molecular formula in solution was first determined by measuring its MW using the cryoscopic method in DMSO/ddw (1 : 49 v/v) (ddw = double distilled water). A solution of 1 μL of **TCNa** (1 mg per 100 μL of DMSO) was diluted to 49 μL of ddw. The molecular weight of **TCNa** was determined to be 573.4 g mol^{-1}, consistent with the calculated value obtained from X-ray analysis. The MW of **TCNa** was found to be 573.4 g mol^{-1} $\{(C_{22}H_{22}N_2O_8)^{2-}2Na^{+}(MeOH)2(H_2O)\}$ (calc. 556.44 g mol^{-1}). Therefore, it can be inferred that the formulation of **TCNa** is retained in the solution.

UV-vis and ^{1}H NMR spectroscopy methods. Methanol and DMSO were selected as solvents for recording UV-vis and ^{1}H NMR spectra, instead of water, to facilitate a comparison between insoluble free TCH_2 and **TCNa**.

Stability studies of TCNa. The stability of **TCNa** was examined through ^{1}H NMR in CD_3OD over a 48-hour period (Fig. S3†). The period of 48 h was chosen for stability testing since the biological experiments require 48 h of incubation with **TCNa**. No changes were observed between the initial ^{1}H NMR spectra and the corresponding ones after 48 h, confirming the retention of **TCNa** in solution.

Table 1 The C–O bond lengths reported for the TCs and OTCs to date in their different forms

Name	CCDC code	Type	C1–O (Å)	C3–O (Å)	C4–O (Å)	C13–O (Å)	Ref.
TCs	**TCNa**	Di-anionic	1.236	1.235	1.285	1.251	[a]
	TCYURT10	Zwitterionic	1.241	1.231	1.316	1.277	14
	TETCYH01	Zwitterionic	1.254	1.244	1.339	1.245	15
	TETCYH10	Zwitterionic	1.262	1.237	1.333	1.237	11
	TETCYH11	Zwitterionic	1.248	1.233	1.347	1.247	16
	TETCYH12	Zwitterionic	1.255	1.233	1.334	1.241	16
Average			1.252 ± 0.007	1.236 ± 0.005	1.334 ± 0.010	1.249 ± 0.014	
OTCs	OXYTET	Neutral	1.274	1.233	1.337	1.304	13
	OXYTET01	Neutral	1.27	1.229	1.34	1.306	12
	OXYTETD	Zwitterionic	1.248	1.25	1.334	1.233	11
	OXTETH10	Zwitterionic	1.277	1.235	1.338	1.236	13
	OTETCB	Cationic	1.333	1.235	1.356	1.264	19
	OXTETK	Di-anionic	1.236	1.261	1.258	1.271	13

[a] This work.

UV-Vis spectroscopy. The UV-Vis absorption spectra of **TCNa** and TCH_2 were recorded in DMSO solution (Fig. S4†). The absorption band at 365 nm ($\log \varepsilon$ = 2.8) in the spectrum of TCH_2 is shifted to 381 nm in the spectrum of **TCNa** ($\log \varepsilon$ = 3.7). The band at 265 nm ($\log \varepsilon$ = 2.8) in the spectrum of TCH_2 remains unshifted in **TCNa** (265 nm, $\log \varepsilon$ = 3.7). These bands are assigned to $\pi^* \leftarrow \pi$ transitions.

^{1}H NMR spectroscopy. The ^{1}H NMR spectra of TCH_2 and **TCNa** in MeOH-d_4 were recorded (Fig. S5†). In the spectrum of TCH_2, the resonance signals at 7.56–7.52, 7.19–7.17 and 6.96–6.94 ppm are assigned to H[$C(18)_{aromatic}$], H[$C(19)_{aromatic}$] and H[$C(17)_{aromatic}$], respectively (Scheme 1).[33] These signals are shifted downfield in the case of the spectrum of **TCNa** at 7.25–7.21 ppm, 6.92–6.90 ppm and 6.71–6.69 ppm, respectively. The resonance signal at 4.13 ppm is assigned to H[OC(8)], which is absent in **TCNa**, due to the deprotonation of the hydroxylic group. The resonance signal of the 6,H[OC(16)],H[OC(15)],H[OC(3)] proton remains unchanged at 4.86 ppm. The resonance signals at 3.06–2.95 ppm in the spectrum of TCH_2 are assigned to the protons of H[C(10)] and they are shifted at 2.74–2.61 ppm in the case of **TCNa**. The signal at 2.29–2.26 ppm in the spectrum of TCH_2 is assigned to the methyl protons of H[$H_3C(20)$] and H[$H_3C(21)$] and it is shifted downfield at 2.07–2.03 ppm in the case of **TCNa**. The signal at 2.00–1.91 ppm is assigned to the H[C(11)] proton in the spectrum of TCH_2 and it is shifted at 1.92–1.88 ppm in the spectrum of **TCNa**. The signal at 1.65 ppm in the spectrum of TCH_2 is assigned to the methyl protons of H[$H_3C(22)$] and it is shifted downfield at 1.49 ppm in the case of **TCNa**. The new signals at 2.38 and 1.31 ppm in the spectrum of **TCNa** are assigned to the coordinated methanol (Fig. S5†).

Biological activity

Antibacterial activity. The antimicrobial efficacy of **TCNa** was assessed through the minimum inhibitory concentration (MIC), minimum bactericidal concentration (MBC), inhibition zone (IZ) and biofilm elimination concentration (BEC) against Gram-negative bacterial strains *Pseudomonas aeruginosa* (*P. aeruginosa*) and *Escherichia coli* (*E. coli*) and the Gram-positive ones *Staphylococcus epidermidis* (*S. epidermidis*) and *Staphylococcus aureus* (*S. aureus*).

Minimum inhibitory concentration (MIC). Since TCH_2 is recommended for the treatment of microbial keratitis (MK), the effectiveness of **TCNa** was assessed against bacteria abundant in MK namely *E. coli*, *P. aeruginosa, S. epidermidis* and *S. aureus* upon their incubation for 20 h.[23,25,27,30,33–35] The MIC values of TCH_2 were previously established.[29]

TCH_2 and **TCNa** were suspended in water for the antibacterial studies. **TCNa** demonstrated superior antimicrobial activity compared to TCH_2, showing an increase of 3.2-fold against *P. aeruginosa*, 14.7-fold against *E. coli*, and 2.4-fold against *S. aureus* (Table 3 and Fig. S6†). However, there was a reduction of 0.4-fold in the MIC value when **TCNa** was utilized in place of TCH_2 against *S. epidermidis*. The MIC values of **TCNa** against Gram-negative bacteria are lower than those against Gram-positive bacteria. It is very interesting that **TCNa** demonstrates nanomolar MIC values against *E. coli* and *S. aureus* (380 and 560 nM, respectively), whereas the corresponding values for TCH_2 against *E. coli* and *S. aureus* are 5600 and 1320 nM, respectively. It is important to note that bacteria such as *E. coli* and *S. aureus*, associated with microbial keratitis, constitute 15% and 5–36% (15%) of bacterial colonies, respectively.[36]

Table 3 Minimum inhibitory concentrations (MICs), minimum bactericidal concentrations (MBCs), inhibition zones (IZs), and biofilm elimination concentration (BEC) of TCNa and TCH_2, against *P. aeruginosa*, *E. coli*, *S. epidermidis* and *S. aureus*. Their IC_{50} values against human corneal epithelial cells (HCECs) are indicated

Compounds	Gram negative		Gram positive		Ref.
	P. aeruginosa	*E. coli*	*S. epidermidis*	*S. aureus*	
MIC (μM)					
TCNa	8.92 ± 1.78	0.38 ± 0.10	87.36 ± 17.40	0.56 ± 0.07	[a]
TCH_2	28.60 ± 4.90	5.60 ± 1.33	37.80 ± 14.06	1.32 ± 0.34	29
MBC (μM)					
TCNa	80.0 ± 0.0	26.00 ± 3.7	330.0 ± 24.0	21.7 ± 3.3	[a]
TCH_2	92.0 ± 18.0	150.0 ± 25.3	171.4 ± 29.1	10.0 ± 0.0	29
MBC/MIC					
TCNa	9.0	68.4	3.8	38.8	[a]
TCH_2	3.2	26.6	4.5	7.6	29
IZ (mm)					
TCNa	15.5 ± 0.9	26.0 ± 3.4	12.6 ± 1.2	35.0 ± 2.4	[a]
TCH_2	15.2 ± 1.4	22.5 ± 0.6	11.8 ± 0.5	34.3 ± 1.8	29
BEC (μM)					
TCNa	704.4 ± 91.2	—	—	959.8 ± 63.5	[a]
TCH_2	427 ± 84	—	—	>2304	29
IC_{50} (μM) HCECs					
TCNa	>300				[a]
TCH_2	>300				[a]

[a] In this work.

Bacteria with MIC values less than 50 μM are classified as susceptible to an antimicrobial agent, whereas those with MIC values exceeding 100 μM are considered resistant.[37] Thus, *P. aeruginosa*, *E. coli* and *S. aureus* exhibit susceptibility to **TCNa**, as the free drug TCH_2 does. However, *S. epidermidis* is considered resistant to **TCNa** (Table 3).

Efforts to determine whether **TCNa** exhibits bactericidal or bacteriostatic properties involved the utilization of the minimum bactericidal concentration (MBC). The MBC value represents the concentration needed to eliminate 99.9% of the initial bacterial inoculum. The MBC values complement MIC, as MIC indicates the minimum concentration of an antimicrobial agent that inhibits growth, while MBC indicates the minimum concentration of the antimicrobial agent that leads to microbial death.[38]

The MBC values for **TCNa** and TCH_2 range from 22 to 330 μM and 10 to 171 μM, respectively, against all tested bacterial strains (Table 3 and Fig. S7†). **TCNa** exhibits lower MBC values against Gram-negative bacteria compared to TCH_2. Conversely, for Gram-positive bacteria, TCH_2 demonstrates lower MBC values than **TCNa**.

To determine whether the formulation can be categorized as bacteriostatic (MBC/MIC ≥ 4), where the organism is inhibited but not killed, or bactericidal (MBC/MIC ≤ 2), where

99.9% of microorganisms are killed, the MBC/MIC ratios were calculated.[22–30,39] For **TCNa**, the MBC/MIC ratios are ≥4, indicating that it can be classified as bacteriostatic. This implies that **TCNa** inhibits the growth of bacteria without causing their death, similar to TCH_2 (Table 3).

The disc diffusion method was additionally employed to evaluate the antimicrobial activity of **TCNa** *vs.* TCH_2 at a concentration of 1 mM against *P. aeruginosa*, *E. coli*, S. *epidermidis* and *S. aureus* (Table 3 and Fig. 2). There was a notable increase in the inhibition zone size compared to the corresponding one of TCH_2 against both Gram-negative and positive bacteria when **TCNa** was used. This confirms the strongest activity of **TCNa** compared to the antibiotic drug, TCH_2. The range of the diameter of the inhibition zones formed by **TCNa** or TCH_2 lies between 12.6 and 35.0 mm and 11.5 and 33.0 mm, respectively (Table 3).

Based on the inhibition zone diameter, bacteria can be categorized into three groups: sensitive if they cause an IZ ≥ 17 mm, intermediate if they cause an IZ between 13 mm and 16 mm, and resistant if the IZ is ≤12 mm.[22–30,39] As a result, *E. coli* and *S. aureus* are characterized as sensitive to both **TCNa** and TCH_2, while *P. aeruginosa* and *S. epidermidis* fall into the category of intermediate sensitivity.

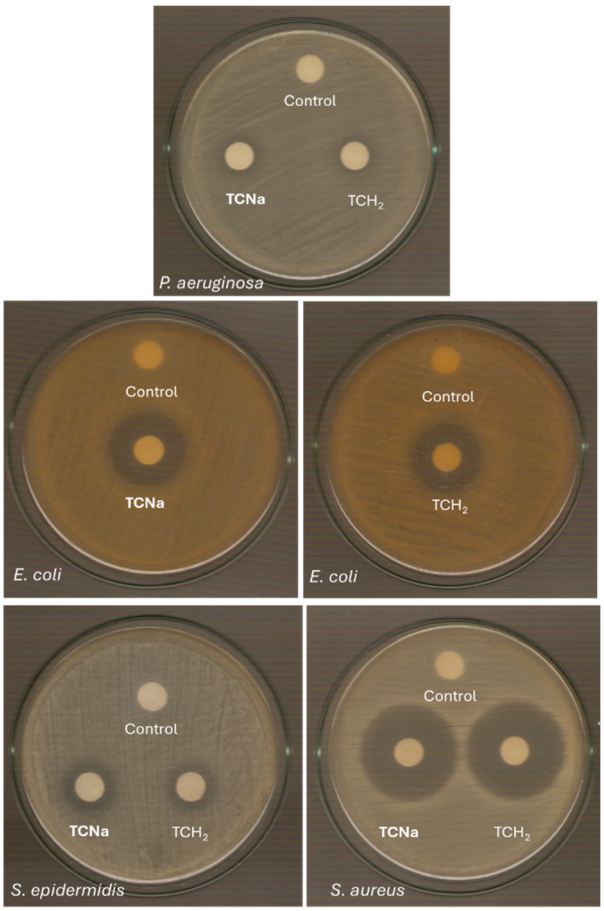

Fig. 2 IZs developed in agar plates of *P. aeruginosa*, *E. coli*, *S. epidermidis* and *S. aureus* by **TCNa** and TCH_2 at 1 mM.

Effect of TCNa on biofilm formation. Eliminating biofilms presents a significant challenge in addressing bacterial infections like those caused by *P. aeruginosa* and *S. aureus* on the cornea. This is particularly crucial as 80% of clinical infections are associated with biofilms. In general, biofilms have demonstrated greater resilience compared to planktonic cell systems, primarily because of their high impermeability to external antimicrobial agents.[40]

The efficacy of **TCNa** in inhibiting biofilm formation was assessed using the biofilm elimination concentration (BEC), while the formation of bacterial biofilms was tracked using crystal violet staining[22–31] (Table 3 and Fig. S8†). The BEC value is defined as the concentration required to achieving a minimum 99.9% reduction in the viability of biofilm-forming bacteria. The BEC values for **TCNa** are 704 and 960 μM, respectively, against *P. aeruginosa* and *S. aureus* (Table 1 and Fig. S8†). **TCNa** demonstrates greater efficiency (up to 2-fold) than TCH_2 against *S. aureus* biofilms, while its efficacy in eliminating *P. aeruginosa* biofilms is lower compared to TCH_2.

Assessment of the *in vitro* toxicity of TCNa on human corneal epithelial cells (HCECs). The initial stage of assessing agent biocompatibility involves cytotoxicity investigations using cell culture-based methods. Cytotoxicity assays provide both qualitative and quantitative assessments of an agent's potential hazard.[41] For bacterial keratitis, employing human corneal epithelial cells (HCECs) appears more suitable, given that human lens epithelial cells are the preferred model for studying intraocular infections.[41]

The cytotoxicity of **TCNa** and TCH_2 was assessed over a 48 hour period, revealing their non-toxic characteristics against HCECs at a concentration of up to 300 μM. According to the ISO 10993-5 guidelines, an agent is considered non-cytotoxic when the percentage of cell viability exceeds 70%.[42] For HCECs treated with **TCNa** and TCH_2, the percentages of viable cells are (83.1 ± 3.5) % and (69.3 ± 4.3)%, respectively, when they are treated with a concentration of 300 μM. Consequently, **TCNa** should be regarded as an *in vitro* non-toxic agent.

Moreover, the selectivity index (SI) serves as a relative indicator of agent safety. The SI is a ratio between the agent dosage inducing toxicity and the dosage producing a therapeutic effect (SI_{MIC} = IC_{50} (against HCECs)/MIC). A higher therapeutic index indicates a greater desired effect compared to undesired cellular toxicity. Conversely, a narrow therapeutic index (low ratio) means there is a small margin between achieving therapeutic success and encountering toxicity.[23,30,43]

The selectivity index (SI) range for **TCNa** is between 3 and 789, whereas for TCH_2, it ranges from 8 to 227. **TCNa** exhibits a higher selectivity index and a more desirable effect compared to TCH_2. Despite the narrower therapeutic window of **TCNa** for *S. epidermidis*, the corresponding ones for *P. aeruginosa*, *E. coli*, and *S. aureus* are 3, 14.7, and 2.4 times higher than that of TCH_2, respectively.

***In vivo* toxicity evaluation by brine shrimp *Artemia salina*.** *Artemia salina*, a zooplanktonic crustacean, is regarded as a model organism for *in vivo* toxicological tests by the United States Environmental Protection Agency (US-EPA).[44,45]

Furthermore, this acute model assay demonstrates a strong correlation with toxicity data obtained from rodents and humans.[44] The survival rates (%) of *Artemia salina* larvae exposed to **TCNa** are assessed at concentrations corresponding to the minimum inhibitory concentration (MIC_{min} = 0.5 μM), observed against the strains tested here, as well as the maximum concentration (MIC_{max} = 150 μM), and twice the maximum concentration (2 × MIC_{max} = 300 μM), over a 24 hour period.

The survival rates are 100.0 ± 0.0, 94.4 ± 6.9 and 71.8 ± 7.0 % for 0.5, 150 and 300 μM concentrations, respectively. Furthermore, the antibiotic TCH_2 has been evaluated at concentrations up to 100 μM, with no observed impact on the survival of *A. salina.*[31] The *in vivo* toxicity results align with those of the *in vitro* studies (see above), as no toxic effects of the substance were observed on human corneal epithelial cells (HCECs) up to a concentration of 300 μM. Similarly, the survival rate of *A salina* exceeds 70% when incubated at 300 μM. This suggests that **TCNa** does not exhibit *in vivo* toxic behavior.

Conclusion

At present, fifty percent of the drug approvals issued by the United States Food and Drug Administration (US FDA) involve pharmaceutical ingredients formulated as salts, and the same percentage of the top 200 prescription drugs consists of pharmaceutical salts.[46] In particular, sodium is among the most commonly preferred cations utilized in oral or parenteral formulations, as well as in topical products.[46] Moreover, 95% of the existing medications for ophthalmic infections are comprised of eye drops and hydrophilic drugs. Water-soluble hydrophilic drugs offer notably higher bioavailability and are more easily administered to the eye in drop form. Consequently, the development of a water-soluble hydrophilic tetracycline formulation is a matter of significant research and technological and financial importance.

Furthermore, the corneal epithelium, conversely, allows only hydrophilic compounds with molecular weights below 500 g mol^{-1} to penetrate due to its paracellular pore diameter of 2.0 ± 0.2 nm.[47]

The chemical characteristics of tetracycline were altered within the compound $\{[TC]^{2-}[Na^{+}(MeOH)(H_2O)]\ [Na^{+}]\cdot(H_2O)\}$ (**TCNa**) to enhance its water solubility and biocompatibility for use in eye drops. In addition, its molecular weight is 556.44 g mol^{-1}, which falls within the range of molecular weights that can permeate the corneal epithelium through paracellular pores.

As a result, **TCNa** was evaluated for the treatment of ophthalmic infections, particularly microbial keratitis. **TCNa** exhibited enhanced antimicrobial efficacy compared to TCH_2, as evidenced by MIC values, showing a 3.2-fold increase against *P. aeruginosa*, a 14.7-fold increase against *E. coli*, and a 2.4-fold increase against S. *aureus*.

The aforementioned bacteria are susceptible to **TCNa**. Moreover, **TCNa** can be categorized as bacteriostatic, indicating that it inhibits the growth of bacteria without causing their death, similarly to TCH_2. The range of the diameter of the inhibition zones of **TCNa** is higher than that of TCH_2. Based on the length of the IZ diameter, *E. coli* and *S. aureus* are characterized as sensitive to both **TCNa** and TCH_2, while *P. aeruginosa* and *S. epidermidis* fall into the category of intermediate sensitivity. **TCNa** demonstrates greater elimination efficiency (up to 2-fold) than TCH_2 against *S. aureus* biofilms.

The biocompatibility of the new formulation was first assessed using an *in vitro* cytotoxicity assay, followed by an *in vivo* cytotoxicity assay using the *Artemia salina* test. The findings confirmed that both **TCNa** and TCH_2 exhibited non-toxicity against HCECs when tested at concentrations of up to 300 μM. This conclusion was drawn from the cell viability percentage exceeding 70%, in accordance with the ISO 10993-5 guidelines. Additionally, the findings from the *in vivo* tests were consistent with those from the *in vitro* studies. Overall, **TCNa** demonstrates a wider therapeutic window, exhibiting a more favorable balance between desirable effects and toxicity compared to TCH_2.

In conclusion, **TCNa** represents a water-soluble, non-toxic bacteriostatic formulation effective against the bacteria associated with microbial keratitis, which have shown susceptibility to **TCNa**. This positions **TCNa** as a potential candidate for the development of new pharmaceutical ingredients for eye drops aimed at treating microbial keratitis.

Experimental

Materials and instruments

All solvents utilized were of reagent grade. The tryptone tryptophan medium, beef extract powder, bacteriological peptone, and soy peptone were procured from Biolife. Agar and yeast extract were acquired from Fluka Analytical. Sodium chloride, D(+)-glucose, dipotassium hydrogen phosphate trihydrate, trichloroacetic acid, and acetic acid were sourced from Merck. Dulbecco's modified Eagle's medium (DMEM), fetal bovine serum, glutamine, and trypsin were obtained from Gibco, Glasgow, UK. Sulforhodamine B was purchased from Alfa Aesar. Phosphate buffer saline (PBS) was acquired from Sigma-Aldrich. Dimethyl sulfoxide was sourced from Riedel-de Haën. Melting points were determined in open tubes using a Stuart Scientific apparatus and remained uncorrected. IR spectra spanning the region of 4000–370 cm^{-1} were recorded using a Cary 670 FTIR spectrometer, Agilent Technologies. The ^{1}H-NMR spectra were captured on a Bruker AC 400 MHz FT-NMR instrument in DMSO-d_6 solution. Electronic absorption spectra were obtained using a UV-1600 PC series spectrophotometer from VWR.

Synthesis of TCNa

0.240 g (0.5 mmol) of tetracycline hydrochloride was dissolved in 10 mL of distilled water (ddH_2O), followed by the addition of 0.5 mL of 1 N KOH (0.5 mmol) solution, resulting in the formation of a yellow precipitate. The precipitate was filtered, dried, and transferred to a flask containing 1.5 mmol NaOH and 1.5 mmol

CS_2 in 20 mL of methanol (MeOH). The mixture was stirred at 0 °C for 3 hours and then filtered. Crystals were observed after two days, dried at room temperature, and stored in a freezer.

TCNa: yield 30%; melting point: >250 °C; elemental analysis found: C: 51.28; H: 5.55; N: 5.64%; calculated for $(C_{23}H_{28}N_2Na_2O_{10})_n$: C: 51.31; H: 5.24; N: 5.20%. IR (cm^{-1}): 3412br, 2935 m, 1610 m, 1578vs, 1465 m, 1420vs, 1361s, 1320 m, 1298 m, 1259 m, 1160 m, 1131 m, 1113 m, 1067 m, 1035 m, 1003s, 971s, 936 m, 877s, 852s, 756s, 697s, 616 m, 596 m, 568 m, 485 m, 462s, 425s; ^{1}H NMR (ppm) in MeOH-d_4: 7.25–7.21 (t, H[C(18)$_{aromatic}$], J = 8.56, 7.58), 6.92–6.90 (d, H[C(19)$_{aromatic}$], J = 7.34), 6.71–6.69 (d, H[C(17)$_{aromatic}$], J = 7.09), 4.89 (s, 6,H[OC(16)],H[OC(15)], H[OC(3)]), 2.74–2.61 (m, H[C(10)]), 2.38 (s, coordinated methanol), 2.07–2.03 (m, H[H_3C(20)] and H[H_3C(21)]), 1.92–1.88 (m, H[C(11)]), 1.49 (s, H[H_3C(22)]), 1.31(s, coordinated methanol); UV-vis (DMSO): λ_{max} = 271 (log ε = 3.8), 369 (log ε = 3.8)

X-ray structure determination

Single crystals of **TCNa** suitable for crystal structure analysis were obtained through slow evaporation of their mother liquids at room temperature. They were then mounted at room temperature on a Bruker Kappa APEX2 diffractometer equipped with a triumph monochromator using MoKα radiation. Unit cell dimensions were determined and refined by utilizing the angular settings of at least 200 high-intensity reflections (>10 $\sigma(I)$) within the range of 2.9 < 2θ < 27.2°. Intensity data were recorded using φ and ω scans. All crystals exhibited no decay during the data collection process. The frames collected for each crystal were integrated using the Bruker SAINT software package[48] using a narrow-frame algorithm. Data were corrected for absorption using the numerical method (SADABS) based on crystal dimensions.[49] The structure was solved using the SUPERFLIP package[50] incorporated into Crystals. Data refinement (full-matrix least-squares methods on F^2) and all subsequent calculations were carried out using the Crystals version 14.40b program package. All non-hydrogen atoms were refined anisotropically. Hydrogen atoms were located by difference maps at their expected positions and refined using soft constraints. By the end of the refinement, they were positioned geometrically using riding constraints to bonded atoms.

TCNa: $C_{23}H_{28}N_2Na_2O_{10}$, H_2O, MW = 556.48, monoclinic, space group $P2_1$, a = 13.701 (7), b = 6.178 (3), c = 14.782 (8) Å, β = 111.527 (12)°, V = 1163.9(10) Å^3, Z = 2, T = 295 K, ρ(calc.) = 1.588 g cm^{-3}, μ = 0.157 mm^{-1}, F(000) = 584. 14 569 reflections measured, 4372 unique (R_{int} = 0.020). The final R_1 = 0.0379 (for 3532 reflections with $I > 2\ s(I)$) and wR(F2) = 0.0562 (all data) S = 1.00 (CCDC 2330616).†

Biological tests

Bacterial strains. For the antibacterial experiments, the strains *Staphylococcus epidermidis* (ATCC® 14990™), *S. aureus* subsp. *aureus* (ATCC® 25923™), *P. aeruginosa* and *Escherichia coli* were used. The Gram-negative bacterial strains *P. aeruginosa* and *Escherichia coli* were kindly donated by the Laboratory of Biochemistry at the University of Ioannina, Greece.

Effect of TCNa on the growth of microbial strains. This study was performed as previously described.[22–30] In short, bacterial strains were streaked onto trypticase soy agar plates and then incubated at 37 °C for 18–24 h. Following incubation, three to five isolated colonies showing similar morphological characteristics were selected from fresh agar plates using a sterile loop and transferred into tubes containing 2 mL of sterile saline solution. The optical density at 620 nm was adjusted to 0.1, corresponding to 10^8 colony-forming units per milliliter (cfu mL^{-1}). The final inoculum size for broth dilution was set at 5 × 10^5 cfu mL^{-1}. Each culture solution, including both the **TCNa**-treated and positive/negative controls, had a total volume of 2 mL. **TCNa** concentrations ranged from 0.05 to 150 μM. After incubation for 20 hours, growth was assessed. The minimal inhibitory concentration (MIC) was determined as the concentration of the compound that inhibits visible bacterial growth. The MIC value was obtained by plotting the optical density of the solution at 620 nm against different concentrations.[22–30]

Minimum bactericidal concentration testing. This study was performed as previously described.[22–30] The bacteria were first cultured with **TCNa** in broth for 20 h. MBC values were determined in duplicate by subculturing 4 μL of the broth onto agar plates. Colony growth indicated non-bactericidal activity of the compound. Therefore, the minimum bactericidal concentration was defined as the lowest concentration at which the tested compound completely inhibited microbial growth.[22–30]

Determination of the inhibition zone (IZ) through the agar disk-diffusion method. This study was performed according to the standard procedure as previously described.[22–30] Subsequently, agar plates were inoculated with a standardized inoculum (at 10^8 cfu ml^{-1}) of the tested microorganism. Filter paper disks (9 mm in diameter), previously soaked with **TCNa** and TCH_2 (at 1 mM concentration), were positioned on the agar surface. The Petri dishes were then incubated for 20 h, after which the diameters of the inhibition zones were measured.[22–30]

Effect of TCNa on biofilm formation. Bacteria at a density of 1.3 × 10^6 cfu mL^{-1} were introduced into LB agar broth medium for *P. aeruginosa* or tryptic soy broth for *S. aureus* (total volume = 1500 μL) in test tubes and incubated for 20 hours at 37 °C. Subsequently, the contents of each test tube were carefully removed, and the tubes were rinsed with 1 mL of 0.9% saline solution followed by the addition of 2 mL of broth. The negative control consisted solely of broth. Next, the bacteria were exposed to **TCNa** at concentrations ranging from 20 to 900 μM for 20 h at 37 °C. The contents of each tube were then poured out and washed three times with 1 mL of methanol and 2 mL of 0.9% saline solution before being left to dry. The tubes were stained with a 0.1% w/v crystal violet solution for 15 minutes. Excess stain was removed by rinsing with 1 mL of methanol and 2 mL of 0.9% saline solution, followed by 3 mL of 0.9% saline solution. The tubes were left to dry for 24 hours, and the bound crystal violet stain was released by

adding 30% glacial acetic acid. The optical density of the resulting solution was then measured at 550 nm to determine the biofilm biomass.[22–30]

Sulforhodamine B assay. These studies were performed in accordance with the previously reported method.[22–30] Briefly, HCECs were seeded in a 96-well plate at a density of 10 000 cells per well and after 24 h of cell incubation, the compounds were added in the concentration range of 50–300 μM for **TCNa** and TCH_2. HCECs were exposed to compounds for a period of 48 h.

Evaluation of toxicity with the brine shrimp assay. The brine shrimp assay was performed as previously described.[22–30] For the toxicity experiments, brine shrimp eggs (*Artemia salina*) were purchased from Ocean Nutrition. Initially, 1 g of cysts was hydrated in freshwater for one hour in a separating funnel or cone-shaped container. Seawater was prepared by dissolving 17 g of sea salt in 500 ml of distilled water. The cone was provided with adequate aeration for 48 hours at room temperature and under continuous illumination. After hatching, nauplii released from the eggshells were gathered at the illuminated side of the cone (near the light source) using a micropipette. The larvae were separated from the eggs by transferring them into small beakers containing 0.9% NaCl solution. An aliquot (0.1 mL) containing approximately 5 to 15 nauplii was dispensed into each well of a 24-well plate, and micelles were added to each well at concentrations corresponding to the minimum inhibitory concentration (MIC_{min} = 0.5 μM), observed against the strains tested here, as well as the maximum concentration (MIC_{max} = 150 μM), and twice the maximum concentration (2 × MIC_{max} = 300 μM), over a 24-hour period. The brine shrimps were observed after 24 hours using a stereoscope. Larvae were considered deceased if they showed no internal or external movement within 10 seconds of observation. Each experiment was repeated three times.

Author contributions

Conceptualization, S. K. Hadjikakou; investigation, A. S. Tsigara, C. N. Banti and A. Hatzidimitriou; methodology, C. N. Banti, A. Hatzidimitriou and S. K. Hadjikakou; supervision and validation, S. K. Hadjikakou; writing – original draft, C. N. Banti and S. K. Hadjikakou; writing – review & editing, C. N. Banti and S. K. Hadjikakou.

Conflicts of interest

The authors declare no conflict of interest.

Acknowledgements

(i) This work was carried out in fulfilment of the requirements for the master thesis of Ms. A. S. T. according to the curriculum of the International Graduate Program in "Biological Inorganic Chemistry", which operates at the University of Ioannina within the collaboration of the Departments of Chemistry of the Universities of Ioannina, Athens, Thessaloniki, Patras, Crete and the Department of Chemistry of the University of Cyprus (https://bic.chem.uoi.gr/BIC-En/index-en.html) under the supervision of Prof. S. K. H. (ii) The International PhD Program, entitled "Biological Inorganic Chemistry (BIC)", is acknowledged. This program is co-financed by Greece and the European Union (European Social Fund – ESF) through the Operational Program "Human Resources Development, Education and Lifelong Learning 2014-2020" in the context of subproject 6 "Biological Inorganic Chemistry (BIC)" (MIS 5162213). This paper was supported by the Special Account for Research Funds (Research Committee) of the University of Ioannina.

References

1 D. Ramdhani, S. A. F. Kusuma, D. Sediana and A. P. H. B. Khumairoh, Comparative study of cefixime and tetracycline as an evaluation policy driven by the antibiotic resistance crisis in Indonesia, *Sci. Rep.*, 2021, **11**, 18461.
2 T. S. B. Møller, G. Liu, H. B. Hartman, M. H. Rau, S. Mortensen, K. Thamsborg, A. E. Johansen, M. O. A. Sommer, L. Guardabassi, M. G. Poolman and J. E. Olsen, Global responses to oxytetracycline treatment in tetracycline-resistant Escherichia coli, *Sci. Rep.*, 2020, **10**, 8438.
3 R. R. Vernhardsdottir, M. S. Magn, L. Hynnekleiv, N. Lagali, D. A. Dartt, J. Vehof, C. J. Jackson and T. P. Utheim, Antibiotic treatment for dry eye disease related to meibomian gland dysfunction and blepharitis – A review, *Ocul. Surf.*, 2022, **26**, 211–221.
4 D. Bremond-Gignac, F. Chiambaretta and S. Milazzo, A European Perspective on Topical Ophthalmic Antibiotics: Current and Evolving Options, *Ophthalmol. Eye Dis.*, 2011, **3**, 29–43.
5 T. J. Federici, The non-antibiotic properties of tetracyclines: Clinical potential in ophthalmic disease, *Pharmacol. Res.*, 2011, **64**, 614–623.
6 R. A. Ralph, Tetracyclines and the treatment of corneal stromal ulceration: A review, *Cornea*, 2000, **19**, 274–277.
7 J. P. Gilbard, *Opthalmic solution with tetracycline for topical treatment of dry eye disease*, Canadian Patent, 2339792C, 2000.
8 R. Vardanyan and V. Hruby, Antibiotics, In *Synthesis of Best-Seller Drugs*, ed R. Vardanyan and V. Hruby, Academic Press, 2016, ch 30, pp. 573–643, ISBN 9780124114920.
9 A. I. Caço, F. Varanda, M. J. Pratas de Melo, A. M. A. Dias, R. Dohrn and I. M. Marrucho, Solubility of Antibiotics in Different Solvents. Part II. Non-Hydrochloride Forms of Tetracycline and Ciprofloxacin, *Ind. Eng. Chem. Res.*, 2008, **47**, 8083–8089.
10 I. Chopra and M. Roberts, Tetracycline Antibiotics: Mode of Action, Applications, Molecular Biology, and Epidemiology

of Bacterial Resistance, *Microbiol. Mol. Biol. Rev.*, 2001, 232–260.

11 J. J. Stezowski, Chemical-Structural Properties of Tetracycline Derivatives. 1. Molecular Structure and Conformation of the Free Base Derivatives, *J. Am. Chem. Soc.*, 1976, **98**, 6012.

12 R. Prewo and J. J. Stezowski, Chemical-Structural Properties of Tetracycline Derivatives. 3. The Integrity of the Conformation of the Nonionized Free Base, *J. Am. Chem. Soc.*, 1977, **99**, 1117.

13 K. H. Jogun and J. J. Stezowski, Chemical-Structural Properties of Tetracycline Derivatives. 2. Coordination and Conformational Aspects of Oxytetracycline Metal Ion Complexation, *J. Am. Chem. Soc.*, 1976, **98**, 6018.

14 G. J. Palenik and M. Mathew, Structural Studies of Tetracyclines. Crystal and Molecular Structure of Tetracycline-Urea Tetrahydrate, *J. Am. Chem. Soc.*, 1978, **100**, 4464.

15 M. R. Caira, L. R. Nassimbeni and J. C. Russell, The crystal and molecular structure of tetracycline hexahydrate, *Acta Crystallogr., Sect. B: Struct. Crystallogr. Cryst. Chem.*, 1977, **33**, 1171.

16 F. W. Heinemann, C. F. Leypold, C. R. Roman, M. O. Schmitt and S. Schneider, X-Ray, Crystallography of Tetracycline, Doxycycline and Sancycline, *J. Chem. Cryst.*, 2013, **43**, 213.

17 K. Kamiya, M. Asai, Y. Wada and M. Nishikawa, Opposite chirality of pillaromycin A to tetracyclines: The X-ray analysis of achromycin hydrochloride, *Experientia*, 1971, **27**, 363.

18 R. Prewo and J. J. Stezowski, Chemical-Structural Properties of Tetracycline Derivatives. 9. 7-Chlorotetracycline Derivatives with Modified Stereochemistry, *J. Am. Chem. Soc.*, 1980, **102**, 7015.

19 K. H. Jogun and J. J. Stezowski, *Cryst. Struct. Commun.*, 1976, **5**, 381.

20 J. Robertson, I. Robertson, P. F. Eiland and R. Pepinsky, X-Ray, Measurements of Terramycin Salts, *J. Am. Chem. Soc.*, 1952, **74**, 841.

21 S. Inouye and Y. Iitaka, Crystallographic data on the molecular complexes of tetracycline salts, *Acta Crystallogr.*, 1964, **17**, 207.

22 I. Sainis, C. N. Banti, A. M. Owczarzak, L. Kyros, N. Kourkoumelis, M. Kubicki and S. K. Hadjikakou, New antibacterial, non-genotoxic materials, derived from the functionalization of the anti-thyroid drug methimazole with silver ions, *J. Inorg. Biochem.*, 2016, **160**, 114–124.

23 I. Milionis, C. N. Banti, I. Sainis, C. P. Raptopoulou, V. Psycharis, N. Kourkoumelis and S. K. Hadjikakou, Silver ciprofloxacin (CIPAG): a successful combination of chemically modified antibiotic in inorganic–organic hybrid, *J. Biol. Inorg. Chem.*, 2018, **23**, 705–723.

24 M.-E. K. Stathopoulou, C. N. Banti, N. Kourkoumelis, A. G. Hatzidimitriou, A. G. Kalampounias and S. K. Hadjikakou, Silver complex of salicylic acid and its hydrogel-cream in wound healing chemotherapy, *J. Inorg. Biochem.*, 2018, **181**, 41–55.

25 M. P. Chrysouli, C. N. Banti, I Milionis, D. Koumasi, C. P. Raptopoulou, V. Psycharis, I. Sainis and S. K. Hadjikakou, A water-soluble silver(I) formulation as an effective disinfectant of contact lenses cases, *Mater. Sci. Eng., C*, 2018, **93**, 902–910.

26 I. Ketikidis, C. N. Banti, N. Kourkoumelis, C. G. Tsiafoulis, C. Papachristodoulou, A. G. Kalampounias and S. K. Hadjikakou, Conjugation of Penicillin-G with Silver(I) Ions Expands Its Antimicrobial Activity against Gram negative Bacteria, *Antibiotics*, 2020, **9**, 25.

27 A. K. Rossos, C. N. Banti, A. Kalampounias, C. Papachristodoulou, K. Kordatos, P. Zoumpoulakis, T. Mavromoustakos, N. Kourkoumelis and S. K. Hadjikakou, pHEMA@AGMNA-1: A novel material for the development of antibacterial contact lens, *Mater. Sci. Eng., C*, 2020, **111**, 110770.

28 M. P. Chrysouli, C. N. Banti, N. Kourkoumelis, E. E. Moushi, A. J. Tasiopoulos, A. Douvalis, C. Papachristodoulou, A. G. Hatzidimitriou, T. Bakas and S. K. Hadjikakou, Ciprofloxacin conjugated to diphenyltin (IV): a novel formulation with enhanced antimicrobial activity, *Dalton Trans.*, 2020, **49**, 11522–11535.

29 A. Meretoudi, C. N. Banti, P. Siafarika, A. G. Kalampounias and S. K. Hadjikakou, Tetracycline Water Soluble Formulations with Enhanced Antimicrobial Activity, *Antibiotics*, 2020, **9**, 845.

30 C. N. Banti, M. Kapetana, C. Papachristodoulou, C. Raptopoulou, V. Psycharis, P. Zoumpoulakis, T. Mavromoustakos and S. K. Hadjikakou, Hydrogels containing water soluble conjugates of silver(I) ions with amino acids, metabolites or natural products for non infectious contact lenses, *Dalton Trans.*, 2021, **50**, 13712–13727.

31 P. Z. Trialoni, Z.-C. M. Fyrigou, C. N. Banti and S. K. Hadjikakou, Conjugation of tetracycline and penicillin with Sb(V) and Ag(I) against breast cancer cells, *Main Group Met. Chem.*, 2022, **45**, 152–168.

32 C. F. Leypold, M. Reiher, G. Brehm, M. O. Schmitt, S. Schneider, P. Matousek and M. Towrie, Tetracycline and derivatives – assignment of IR and Raman spectra via DFT calculations, *Phys. Chem.*, 2003, **5**, 1149–1157.

33 D. E. Williamson and G. W. Jr Everett, A proton nuclear magnetic resonance study of the site of metal binding in tetracycline, *J. Am. Chem. Soc.*, 1975, **97**, 2397–2407.

34 K. F. Tabbara, H. F. El-Sheikh and B. Aabed, Extended wear contact lens related bacterial keratitis, *Br. J. Ophthalmol.*, 2001, **85**, 842–847.

35 F. Stapleton and N. Carnt, Contact lens-related microbial keratitis: how have epidemiology and genetics helped us with pathogenesis and prophylaxis, *Eye*, 2012, **26**, 185–193.

36 D. S. J. Ting, C. S. Ho, R. Deshmukh, D. G. Said and H. S. Dua, Infectious keratitis: an update on epidemiology, causative microorganisms, risk factors, and antimicrobial resistance, *Eye*, 2021, **35**, 1084–1101.

37 D. L. Shungu, E. Weinberg and H. H. Gadebusch, Tentative interpretive standards for disk diffusion susceptibility

testing with norfloxacin (MK-0366, AM-715), *Antimicrob. Agents Chemother.*, 1983, **23**, 256–260.

38 M. Azizi-Lalabadi, A. Ehsani, B. Divband and M. Alizadeh-Sani, Antimicrobial activity of Titanium dioxide and Zinc oxide nanoparticles supported in 4A zeolite and evaluation the morphological characteristic, *Sci. Rep.*, 2019, **9**, 17439.

39 M. Motyl, K. Dorso, J. Barrett and R. Giacobbe, Basic microbiological techniques used in antibacterial drug discovery. In *Current protocols in pharmacology* unit 13A.3.1–13A.3.22, Wiley, New York, 2005.

40 Q. Yang, K. Olaifa, F. P. Andrew, P. A. Ajibade, O. M. Ajunwa and E. Marsili, Assessment of physiological and electrochemical effects of a repurposed zinc dithiocarbamate complex on Acinetobacter baumannii biofilms, *Sci. Rep.*, 2022, **12**, 11701.

41 M. Bernard, E. Jubeli, M. D. Pungente and N. Yagoubi, Biocompatibility of polymer-based biomaterials and medical devices – regulations, in vitro screening and risk-management, *Biomater. Sci.*, 2018, **6**, 2025–2053.

42 C. Koski, N. Sarkar and S. Bose, Cytotoxic and osteogenic effects of crocin and bicarbonate from calcium phosphates for potential chemopreventative and anti-inflammatory applications In Vitro and In Vivo, *J. Mater. Chem. B*, 2020, **8**, 2048–2062.

43 T. M. Rawson, R. C. Wilson, D. O'Hare, P. Herrero, A. Kambugu, M. Lamorde, M. Ellington, P. Georgiou, A. Cass, W. W. Hope and A. H. Holmes, Optimizing antimicrobial use: challenges, advances and opportunities, *Nat. Rev. Microbiol.*, 2021, **19**, 747–758.

44 C. N. Banti and S. K. Hadjikakou, Evaluation of Genotoxicity by Micronucleus Assay in vitro and by Allium cepa Test in vivo, *Bio-Protoc.*, 2019, **9**, e3311.

45 A. Shokry, M. Khalil, H. Ibrahim, M. Soliman and S. Ebrahim, Acute toxicity assessment of polyaniline/Ag nanoparticles/graphene oxide quantum dots on Cypridopsis vidua and Artemia salina, *Sci. Rep.*, 2021, **11**, 5336.

46 D. Gupta, D. Bhatia, V. Dave, V. Sutariya and S. V. Gupta, Salts of Therapeutic Agents: Chemical, Physicochemical, and Biological Considerations, *Molecules*, 2018, **23**, 1719.

47 M. Löscher, C. Seiz, J. Hurst and S. Schnichels, Topical Drug Delivery to the Posterior Segment of the Eye, *Pharmaceutics*, 2022, **14**, 134.

48 Bruker Analytical X-ray Systems, Inc., *Apex2, Version 2 User Manual, M86-E01078*, Madison WI, 2006.

49 Siemens Industrial Automation, Inc., *SADABS: Area–Detector Absorption Correction*, Madison, WI, 1996.

50 L. Palatinus and G. Chapuis, SUPERFLIP – a computer program for the solution of crystal structures by charge flipping in arbitrary dimensions, *J. Appl. Cryst.*, 2007, **40**, 786–790.